

## Specific Features of the Porous Polymeric Particle Composites Application As Fillers for Electrorheological Fluids

N. M. Kuznetsov<sup>a,\*</sup>, V. V. Kovaleva<sup>a</sup>, Y. D. Zagoskin<sup>a</sup>, A. Yu. Vdovichenko<sup>a,b</sup>, S. N. Malakhov<sup>a</sup>, E. V. Yastremsky<sup>a,c</sup>, R. A. Kamyshinsky<sup>a,c,d</sup>, T. E. Grigoriev<sup>a,c</sup>, and S. N. Chvalun<sup>a,b</sup>

<sup>a</sup> National Research Center “Kurchatov Institute”, Moscow, 123182 Russia

<sup>b</sup> Enikolopov Institute of Synthetic Polymeric Materials, Russian Academy of Sciences, Moscow, 117393 Russia

<sup>c</sup> Moscow Institute of Physics and Technology (National Research University), Dolgoprudny, Moscow oblast, 141701 Russia

<sup>d</sup> Shubnikov Institute of Crystallography, Federal Research Center “Crystallography and Photonics”, Russian Academy of Sciences, Moscow, 119333 Russia

\*e-mail: kyz993@yandex.ru

Received March 23, 2021; revised March 23, 2021; accepted April 1, 2021

**Abstract**—The rheological behavior of 1-wt % suspensions filled with composite polymer particles of chitosan with cellulose in polydimethylsiloxane without and in an electric field is studied. The features of the electro-rheological response of the suspensions depending on the filler composition are revealed. The mechanism of the electrorheological effect changes for fillers with a high cellulose content at a field strength higher than 4 kV/mm. The nature of the electrorheological effect is considered from the standpoint of the electrophysical characteristics of suspensions. The results of sedimentation tests are consistent with the rheological data and are determined by the structural features of the composite fillers. The relative efficiency of the studied fluids reaches 10<sup>5</sup>%.

DOI: 10.1134/S2635167621060148

### INTRODUCTION

The active development of science and technology in the 21st century, and the design of new devices and technologies require the creation of materials that combine various functional properties. A large class of such materials are “smart” materials that reversibly change their properties under external stimuli [1]. In recent decades, smart materials have attracted the attention of researchers on account of the possibility of their wide use in mechanics, soft robotics as an alternative to existing “hard” analogs, optics, camouflage, and medicine.

Electrorheological fluids (ERFs) change their rheological behavior (viscosity, yield stress, storage modulus, etc.) under an electric field and are an illustrative example of smart materials. Usually, ERFs are dispersed systems consisting of a liquid nonconductive medium and polarizable microparticles or nanoparticles of a filler [2]. Low-molecular-weight organosilicon polymers (silicone oils with low dielectric permittivity, thermal stability, low cost, and availability in a wide range of molecular weights (viscosities)) are widely used as a dispersion medium [3]. When an electric potential is applied, the filler particles are polarized and form columnar percolation structures between the electrodes: the transition from viscous to elastic behavior is observed. Due to the reversibility of

their properties, ERFs are used in dampers with adjustable stiffness, valves, tactile elements, sensors, robotics, microfluidics, etc. [4].

The ERF efficiency depends on various parameters, such as the nature and viscosity of the dispersion medium [5, 6], the nature and shape of filler particles [7, 8], the presence of activators [9, 10], and the electrophysical characteristics of components [11, 12]. Recent studies are aimed at creating fluids with a low concentration of dispersed phase particles exhibiting a more contrasting change in the rheological properties in an electric field [13, 14]. The formation of a percolation network plays an essential role in such fluids. In this regard, particles with a high aspect ratio [15, 16], as well as fillers prone to self-organization into branched fractal structures [17], are extremely promising.

Polymer and polymer–composite particles are a separate class of fillers for ERFs [18, 19]. The use of natural polymers such as chitosan and cellulose opens up prospects for creating environmentally friendly materials to restore balance between the technosphere and biosphere.

Cellulose is the most abundant biopolymer on Earth; it is a linear polysaccharide chain made up of hundreds and thousands of linked  $\beta$ -1,4-D-glucose units [20]. Cellulose is the main component of the plant cell wall and can be isolated from various agri-

cultural wastes, such as wheat husks, straw and soybeans, coconut-husk fibers, mulberries, etc. Chitin is the second most abundant biopolymer after cellulose. This is a nitrogen-containing polysaccharide, a polymer consisting of N-acetylglucosamine units linked through  $\beta$ -(1 $\rightarrow$ 4)-glycosidic bonds [21]. Chitin particles have intramolecular and intermolecular bonds between acetamide and hydroxyl groups, which determines their high crystallinity. Chitin can be produced at a relatively low cost from organic resources such as crustacean shells (shrimp, lobster, crabs, and krill) and seafood waste. Chitin and cellulose occur in nature in the form of complex hierarchical structures, i.e., fibrils consisting of crystalline and amorphous regions, and can be isolated as separate crystalline domains, i.e., nanocrystals [22]. Chitosan is N-deacetylated chitin. The degree of deacetylation significantly affects the characteristics of chitosan, including its electrorheological activity [23]. It has recently been found that highly porous chitosan particles exhibit a high electrorheological response in various dispersion media at extremely low concentrations (less than 1 wt % (0.62 vol %) [24, 25].

Polymer nanocomposites exhibit unique properties due to the combination of matrix and filler qualities. The introduction of a functional additive into the polymer leads to an increase in the Maxwell–Wagner–Sillars polarization at the interface [26] and can enhance the electrorheological effect. In this work, we study the effect of the composition of composite particles based on chitosan and cellulose nanocrystals on the electrorheological behavior of their suspensions in polydimethylsiloxane.

## EXPERIMENTAL

Polydimethylsiloxane (PMS 100, Penta Junior LLC, Russia) was used as the dispersion medium. The molecular-weight characteristics according to size-exclusion chromatography were as follows:  $M_w = 12.2$  kDa, polydispersity index 2.0.

Composite fillers were obtained from ChitoClear 43000–HQG 10 chitosan (Primex, Iceland;  $M_n = 80$  kDa [27]) and cellulose nanoparticles (nanofibrillar cellulose, Nanografi Nanotechnology AS, Turkey).

Deionized water with the specific electrical conductivity  $\leq 10^{-4}$  S/cm, obtained in a Millipore MilliQ system (Merck KGaA, Germany), and acetic acid (Component reaktiv LLC, Russia) were used as supplementary materials.

*Samples preparation.* Composite particles were obtained similarly to the procedure described in [28]. To obtain ERF fillers, 1-wt % chitosan solution in 1-wt % acetic-acid solution was prepared. Then, nanocellulose particles were dispersed into the solution to obtain suspensions with different concentrations of nanocellulose relative to the solution (0.01, 0.1, 1, 2, and 5 wt %). The resulting suspensions were sonicated with a

UP400S submersible homogenizer (Hielscher Ultrasonics, Germany) for 5 min (400 W, 24 kHz; amplitude 20%). After homogenization, the suspensions were sputtered into a liquid nitrogen bath to form composite particles. The particles were collected and kept in a freezer at  $-24^\circ\text{C}$  for 24 h. The solvent was removed from the pores by lyophilization in an Alpha 2–4 LDplus freeze dryer (Martin Christ, Germany) for 3 days at a pressure in the working chamber of 0.250 mbar, followed by drying for 10 h at a pressure of 0.030 mbar. This technique makes it possible to obtain particles with a high porosity. Thus, composite fillers cellulose/chitosan with different component ratios (designated below in accordance with the cellulose content as 0.01/1, 0.1/1, 1/1, 2/1, and 5/1) were obtained.

ERFs were obtained by mechanical mixing of the selected type of filler with polydimethylsiloxane using an MR Hei-Tec magnetic stirrer (Heidolph, Germany) for 48 h until uniform suspensions were formed. The filler concentration in all the samples was 1 wt %. Before measurements, the fluids were additionally sonicated for 20 min in a UZV-4.0/1 TTTs (RMD) ultrasonic bath (150 W, 35 kHz) (Sapfir LLC, Russia).

*IR spectroscopy.* The composition of the composite fillers and initial polysaccharides was studied by infrared (IR) spectroscopy in a Nicolet iS5 FTIR spectrometer (ThermoFisher Scientific, United States) using an iD5 ATR attenuated total reflectance adapter. The study was performed in the range of 550–4000  $\text{cm}^{-1}$ .

*Rheology.* The rheological behavior of the suspensions without and in an electric field was studied by rotational viscometry in the geometry of coaxial cylinders on a Physica MCR 501 rheometer (Anton Paar, Germany). The cell volume was 20 mL and the gap was 1 mm. An electric potential in the range up to 7 kV was supplied from an HCP 14-12500 MOD external high voltage source (FuG Elektronik GmbH, Germany). Measurements were performed in the controlled shear rate (CSR) mode to obtain flow and viscosity curves, in the controlled shear stress (CSS) mode to determine the yield stress values, and in the oscillatory mode (FS) at a deformation value of 0.1% (linear range) to determine the frequency sweeps of the storage and loss moduli. The measurements were performed at  $20^\circ\text{C}$ .

*Scanning electron microscopy (SEM).* The morphology of the fillers was studied using a SEM Versa 3D instrument (ThermoFisher Scientific, United States). Images were obtained in the high-vacuum mode using an ETD secondary electron detector (ThermoFisher Scientific, United States) at an accelerating voltage of 2 kV and a current of 33 pA. To minimize the accumulation of electric charge, a thin layer of gold was preliminarily sputtered onto the surface of the samples. Micrographs of the particles were also obtained using a Phenom XL SEM instrument

(ThermoFisher Scientific, United States) in the low-vacuum mode (pressure 10 Pa) at an accelerating voltage of 5 kV using a backscattered electron detector without sputtering the conductive coating.

**Transmission electron microscopy (TEM).** The morphology of nanocellulose in an aqueous solution was studied by TEM using a Titan 80-300 instrument (ThermoFisher Scientific, United States) at an accelerating voltage of 300 kV. The samples for TEM studies were prepared using negative staining: at the first stage, the surface of copper grids with a carbon substrate Pelco Pure C (Ted Pella Inc., United States) was hydrophilized using a glow discharge in a Pelco Easi-Glow system (Ted Pella Inc., United States) for 30 s at a current of 25 mA and a pressure of 0.26 mbar. Then, using 1-wt % uranyl acetate solution (Ted Pella Inc., United States), a negative staining procedure was performed in accordance with the protocol in [29].

**Dielectric measurements.** The electrophysical characteristics of the suspensions were obtained using a Novocontrol Alpha-A impedance analyzer (Novocontrol Technologies GmbH & Co. KG, Germany) equipped with a ZGS Alpha Active Sample Cell. The measurements were performed in a special BDS1308 liquid cell consisting of a brass cup with two disk electrodes 20 mm in diameter separated by a fluoroplastic spacer. The distance between the electrodes was 2 mm. The suspension sample was poured into the cup and the liquid cell was placed between the electrodes of the ZGS cell. The measurements were carried out at an effective voltage of 1 V and a temperature of 20°C.

**Sedimentation.** The stability of the suspensions was determined by evaluating the sedimentation ratio of the height of the fluid containing the colloidal phase to the height of the entire fluid column over time. This technique is used to qualitatively assess the stability of suspensions in cases where sedimentation proceeds for a long time and the plotting of classical particle-size distribution functions is impossible or extremely difficult.

## RESULTS AND DISCUSSION

The chemical structure of composite fillers and their components was confirmed by IR spectroscopy (Fig. 1). As noted above, chitosan and cellulose belong to the class of polysaccharides and have a similar structure; therefore, their spectra have a small number of non-overlapping absorption bands suitable for analysis. As can be seen from the presented data, as the cellulose content in the composite particles increases, the intensity of the absorption band of chitosan (Amide I, 1647  $\text{cm}^{-1}$ ) decreases, and the intensity of the cellulose bands at 1110 and 1205  $\text{cm}^{-1}$  increases. In addition, changes are observed in the range of C–H stretching vibrations (2800–3000  $\text{cm}^{-1}$ ): a transition from two absorption bands at 2875 and 2920  $\text{cm}^{-1}$  (typical of chitosan) to one broad band with a maxi-

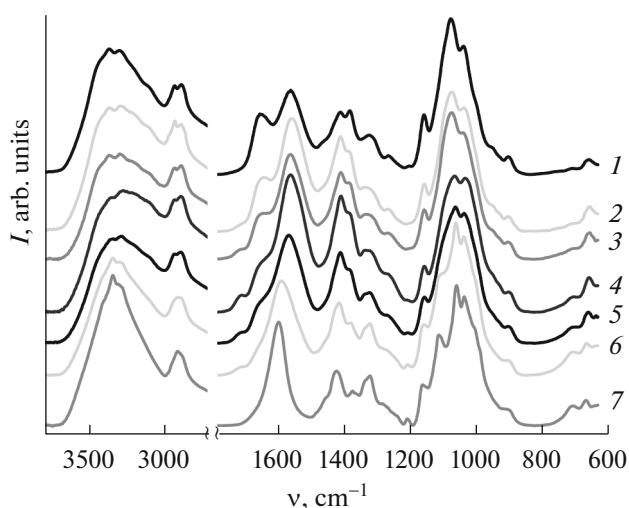


**Fig. 1.** IR spectra of the initial chitosan (1), nanocellulose (7), and porous composite particles of the compositions 0.01/1 (2), 0.1/1 (3), 1/1 (4), 2/1 (5), and 5/1 (6).

imum at 2900  $\text{cm}^{-1}$  can be seen. For composite particles, a component ratio-dependent shift of the absorption-band maximum in the region of 1550–1600  $\text{cm}^{-1}$  occurs due to superposition of the bands of chitosan (Amide I) at 1554  $\text{cm}^{-1}$  and cellulose at 1594  $\text{cm}^{-1}$ . Thus, the data of IR spectroscopy confirmed the presence of both polysaccharides in the composite fillers, as well as their different content.

All the studied suspensions of composite particles in polydimethylsiloxane exhibit an electrorheological effect. In an electric field, a significant increase in the shear-stress values is observed: the yield-stress values increase. The flow and viscosity curves for a suspension filled with particles of the composition 0.1/1 at various electric-field strengths are shown in Fig. 2 as an example. When the potential is applied (Fig. 2a), an increase in the yield-stress values by several orders of magnitude can be seen on the flow curves, as evidenced by a weak change in the shear stress with an increase in the shear rate in a wide range. The corresponding viscosity curves are descending, reaching a plateau at high shear rates (Fig. 2b). We note that the viscosity values also depend on the electric-field strength.

The yield stress is one of the main characteristics of ERF. Figure 3 shows the dependences of the yield stress on the electric-field strength for all fluids studied. The slope of the dependence ( $k$ ) in double logarithmic coordinates depends on the mechanism of the electrorheological effect and is equal to 2 for the polarization mechanism. It is known that the difference between the conductivities of the dispersed phase and the dispersion medium can also affect the behavior of fluids and leads to a change in the slope of the dependence down to 1.5 and even to 1 at polarization saturation [30, 31]. For the fluids studied, a number of

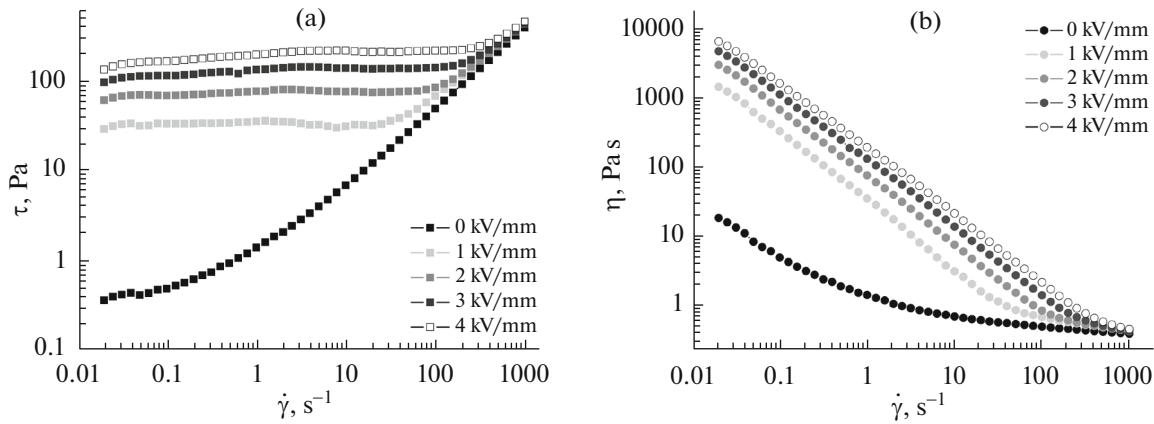


**Fig. 2.** Flow (a) and viscosity (b) curves of a suspension filled with nanocellulose/chitosan composite particles of the composition 0.1/1 at different electric-field strengths.

peculiarities are observed in the plot. For example, the suspensions containing composite particles with a low cellulose content (0.01/1 and 0.1/1) have similar yield-stress values and a dependence proportional to 1.4 over the entire investigated range of electric-field-strength values. This dependence is typical for suspensions of non-composite porous chitosan particles and indicates a predominantly conductive mechanism of the electrorheological effect [24]. As the concentration of cellulose in the composite particles increased, the nature of the dependence changed: for fillers of the composition 1/1, 2/1, and 5/1, a change in the proportionality from 1.3 to 1.0 was observed with an increase in the field strength above 4 kV/mm, which indicates a change in the mechanism of the effect and its more complex nature. The higher yield-stress values for the suspensions filled with composite particles with a low cellulose content should also be noted.

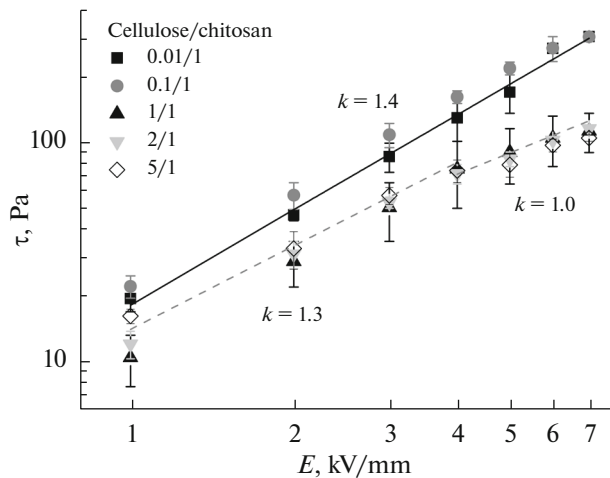


**Fig. 3.** Dependence of the values of the static yield stress on the electric-field strength for suspensions filled with particles of various compositions.

To determine the contribution of viscous and elastic components to the behavior of the samples, the frequency dependences of the storage and loss moduli without and in an electric field were obtained. The data for a fluid filled with particles of the composition 0.1/1 are shown as an example (Fig. 4). Even without an electric field, the storage modulus exceeded the loss modulus in almost the entire frequency range studied, which indicates the prevalence of the elastic component in the sample and confirms the presence of a low yield stress. When an electric field was applied, the values of both moduli sharply increased by several orders of magnitude and only slightly depended on the frequency. We note that the storage modulus exceeded the loss modulus by almost one order of magnitude: in an electric field, the elastic component dominated over the viscous component, confirming the formation of a strong percolation network of filler particles. Interestingly, the values of the moduli decreased with an increase in the proportion of cellulose in the composite particles (data not shown). Thus, the results are consistent with the rheological data obtained in the flow mode.

The nature of the electrorheological effect is associated with a difference in the electrophysical characteristics (dielectric permittivity and conductivity) of the filler and the dispersion medium. The dielectric permittivity and conductivity of polydimethylsiloxane have been repeatedly determined previously and at a frequency of 1 Hz are  $\sim 2.3$  arb. units and  $\sim 10^{-14}$  S/cm, respectively [12, 32]. When polydimethylsiloxane is filled with composite particles, the values of the electrophysical characteristics increase (Table 1).

It can be seen that the values pass through a minimum at a filler composition of 1/1. The high values of the conductivity and dielectric permittivity at a low cellulose content are determined mainly by the porous branched structure of low-density chitosan due to the fact that the surface conductivity in the polymers significantly exceeds the bulk conductivity. An increase

in the cellulose content in the filler structure leads to a decrease in the mass fraction of chitosan and an increase in the fraction of denser cellulose crystals and is reflected in the electrophysical characteristics. For suspensions with fillers of the composition 2/1 and 5/1, the contribution of cellulose exceeds the contribution of chitosan, and an increase in the parameters is observed. Nevertheless, the dielectric permittivity and conductivity values of all the suspensions studied were higher than those of the dispersion medium, which determines the electrorheological response of the fluids.

To identify the factors that cause different rheological behavior and the electrorheological response of fluids with fillers of various compositions, the morphology of filler particles was studied. The initial cellulose powder consisted of micron-sized fibrils (Fig. 5a). However, when a small amount of powder is dispersed into water, the macrostructure undergoes degradation to individual nanocrystals with a high aspect ratio (Fig. 5a, inset). Lyophilization of the filler with a low cellulose content (compositions 0.01/1 and 0.1/1) leads to the formation of polydisperse, predominantly spherical particles with a high porosity (Figs. 5b, 5c). Due to the low contrast between cellulose and chitosan, it is impossible to distinguish nanocrystals in the polymer particle structure in SEM images. With an increase in the cellulose content, the morphology of the particles is disturbed; among the chitosan matrix, large macrofibrils are observed, the number of which increases with concentration (Figs. 5d, 5e). Obviously, the higher the cellulose content in the matrix solution for particle formation, the worse cellulose is dispersed to individual nanocrystals. The problem of cellulose homogenization is reflected in the disturbance of the morphology of filler particles and, at high concentrations, apparently leads to destruction of the composite structure in the ERF composition. For example, in fluids filled with particles of the composition 1/1, 2/1, and 5/1, several types of particles are simultaneously present: shapeless porous chitosan fragments, macrofibrils, and cellulose nanocrystals. This, in turn, leads to a decrease in the yield stress as well as storage and loss moduli of ERF in an electric field and explains the change in the mechanism of the electrorheological effect in high-power electric fields (Fig. 2).

The peculiarities of the structure of composite fillers, depending on the cellulose content, are reflected in the sedimentation stability of ERFs. Figure 6 shows the dependence of the sedimentation ratio over time. Fluids containing composite fillers of the compositions 0.01/1 and 0.1/1 retain high sedimentation stability similarly to non-composite porous particles [24]. The sedimentation ratio exceeded 95% after approximately 100 h of observation. Such stability is associated with the formation of an extended colloidal structure from porous filler particles due to the penetration of dispersion-medium molecules into the pores in the

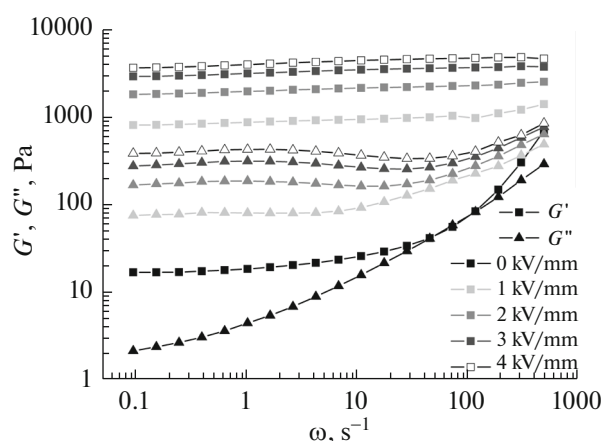


**Fig. 4.** Frequency dependences of the storage modulus ( $G'$ ) and loss modulus ( $G''$ ) of a suspension filled with nanocellulose/chitosan composite particles of the composition 0.1/1 at different electric-field strengths.

particles. The worst sedimentation stability was exhibited by suspensions with a filler of the composition 5/1: the sedimentation ratio drastically decreased in the first 2 h of observation and reached a constant value of  $\sim 18\%$  in just 4 h. Fluids filled with composite particles of the composition 1/1 and 2/1 occupy an

**Table 1.** Electrophysical characteristics of suspensions at a frequency of 1 Hz

Filler composition	$\epsilon$ , arb. units	$\sigma \times 10^{13}$ , S/cm
0.01/1	4.94	11.4
0.1/1	3.83	8.12
1/1	3.02	1.62
2/1	3.25	2.55
5/1	4.03	2.98

**Table 2.** Relative efficiency of electrorheological fluids filled with composite polymeric particles of various compositions

Filler composition	0.01/1	0.1/1	1/1*	2/1*	5/1*
	$Ef_{\text{rel}} \times 10^{-2}$ , %				
1	3	29	104	120	162
2	9	77	287	310	329
3	18	146	507	534	576
4	28	217	761	724	748
5	37	294	906	845	795
6	49	363	1054	1029	976
7	66	409	1136	1162	1054

\*In the case of suspensions that do not have a yield stress without an electric field, the relative efficiency was estimated using the shear-stress value of 0.1 Pa as the  $\tau_0$  parameter.



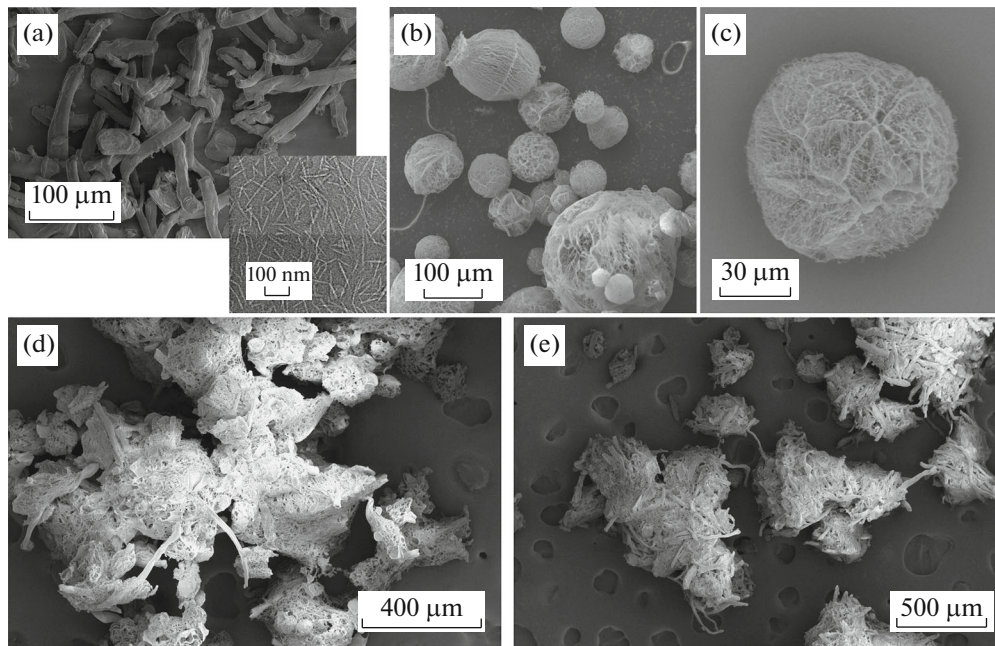


**Fig. 5.** SEM images of the initial cellulose particles (a), nanocellulose/chitosan porous composite particles of the composition 0.1/1 at various magnifications (b, c), as well as particles of the composition 2/1 (d) and 5/1 (e). The inset (a) shows a TEM image of 0.1-wt % suspension of nanocellulose in water.

intermediate position in terms of stability: the ratio reached a constant value within 8–10 h and was ~30%. Apparently, fluids with a high cellulose content in the filler are less stable due to destruction of the porous structure of chitosan and the presence of large particles (cellulose macrofibrils).

The relative efficiency of ERF reflects the contrast of changes in the rheological behavior and can be calculated by the formula [33]:

$$Ef_{rel} = ((\tau_E - \tau_0)/\tau_0) \times 100\%,$$

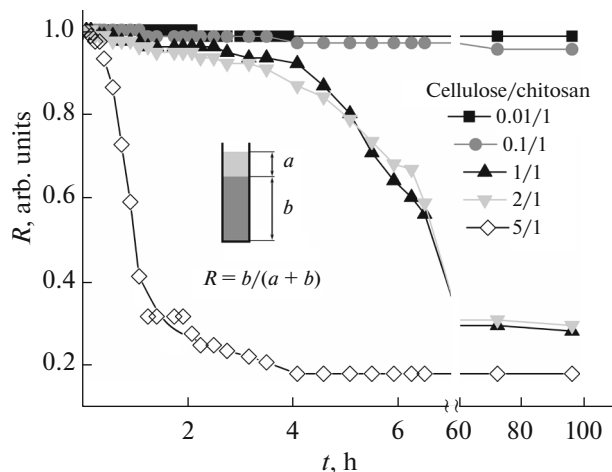


**Fig. 6.** Sedimentation stability of suspensions filled with particles of various compositions.

where  $Ef_{rel}$  is the relative efficiency,  $\tau_E$  is the value of the yield stress of the suspension in an electric field, and  $\tau_0$  is the value of the yield stress without an electric field. The values of the relative efficiency of fluids filled with composite particles of various compositions are shown in Table 2.

The relative efficiency of fluids increases with an increase in the electric-field strength and cellulose content in the filler and reaches approximately 10<sup>5</sup>%. Thus, despite the lower sedimentation stability and reduced yield stress of suspensions in an electric field, the relative efficiency of suspensions with a high cellulose content in the composite (1/1, 2/1, and 5/1) is extremely high.

## CONCLUSIONS

The efficiency of composite polymer fillers with a high porosity for ERFs is shown. The important parameters that determine the magnitude of the electrorheological response of the studied suspensions and their sedimentation stability are the quality and homogeneity of the distribution of cellulose particles in the composite filler. The principal possibility to change the properties of ERF by varying the composition of the filler in order to create smart materials with desired properties is shown. Understanding the relationship between the functional characteristics of fluids and the structural organization of the filler allows an expanded notion of the nature of the electrorheological effect and to purposefully change the properties of the material.

## ACKNOWLEDGMENTS

The analysis of the molecular-weight characteristics of polydimethylsiloxane was performed at the Collaborative Access Center “Center for Polymer Research” of the Enikolopov Institute of Synthetic Polymeric Materials, Russian Academy of Sciences. We express our gratitude to the resource centers Nanozond, Elektrofizika, Polymer, and Optika of the National Research Center “Kurchatov Institute”, for the opportunity to perform electron microscopic, dielectric spectroscopic, and rheological studies.

## FUNDING

The study was supported by the Russian Science Foundation (project no. 20-73-00205).

## CONFLICT OF INTEREST

The authors declare that they have no conflicts of interest.

## REFERENCES

- M. A. C. Stuart, W. T. S. Huck, J. Genzer, et al., *Nat. Mater.* **9**, 101 (2010).  
<https://doi.org/10.1038/nmat2614>
- T. Hao, *Adv. Mater.* **13**, 1847 (2001).  
[https://doi.org/10.1002/1521-4095\(200112\)13:24<1847::AID-ADMA1847>3.0.CO;2-A](https://doi.org/10.1002/1521-4095(200112)13:24<1847::AID-ADMA1847>3.0.CO;2-A)
- M. J. Owen, in *Encyclopedia of Materials: Science and Technology*, Ed. by K. H. J. Buschow et al. (Elsevier, Amsterdam, 2001), p. 2480.  
<https://doi.org/10.1016/B0-08-043152-6/00448-4>
- Y. Z. Dong, Y. Seo, and H. J. Choi, *Soft Matter* **15**, 3473 (2019).  
<https://doi.org/10.1039/c9sm00210c>
- Y. Hong and W. Wen, *J. Intell. Mater. Syst. Struct.*, **1** (2015).  
<https://doi.org/10.1177/1045389X15596623>
- O. I. Davydova, A. S. Kraev, A. A. Redozubov, T. A. Trusova, and A. V. Agafonov, *Russ. J. Phys. Chem. A* **90**, 1269 (2016).  
<https://doi.org/10.1134/S0036024416060054>
- M. M. Ramos-Tejada, J. M. Rodriguez, and A. V. Delgado, *Rheol. Acta* **57**, 405 (2018).  
<https://doi.org/10.1007/s00397-018-1086-8>
- A. V. Agafonov, A. S. Kraev, O. S. Ivanova, et al., *Rheol. Acta* **57**, 307 (2018).  
<https://doi.org/10.1007/s00397-018-1076-x>
- A. V. Agafonov, O. I. Davydova, A. S. Krayev, et al., *J. Phys. Chem. B* **121**, 6732 (2017).  
<https://doi.org/10.1021/acs.jpcc.7b04131>
- Y. Liang, X. Yuan, L. Wang, et al., *J. Colloid Interface Sci.* **564**, 381 (2020).  
<https://doi.org/10.1016/j.jcis.2019.12.129>
- N. M. Kuznetsov, V. G. Shevchenko, D. Y. Stolyarova, et al., *J. Appl. Polym. Sci.* **135**, 46614 (2018).  
<https://doi.org/10.1002/app.46614>
- N. M. Kuznetsov, V. G. Shevchenko, S. I. Belousov, and S. N. Chvalun, *Russ. J. Phys. Chem. A* **94**, 376 (2020).  
<https://doi.org/10.1134/S003602442002020X>
- D. Y. Stolyarova, N. M. Kuznetsov, S. I. Belousov, and S. N. Chvalun, *J. Appl. Polym. Sci.* **136**, 47678 (2019).  
<https://doi.org/10.1002/app.47678>
- A. V. Agafonov, A. S. Kraev, M. A. Teplonogova, et al., *Rheol. Acta* **58**, 719 (2019).  
<https://doi.org/10.1007/s00397-019-01175-7>
- N. M. Kuznetsov, S. I. Belousov, N. P. Bessonova, and S. N. Chvalun, *Izv. Vyssh. Uchebn. Zaved., Khim. Khim. Tekhnol.* **61**, 61 (2018).  
<https://doi.org/10.6060/tcct.20186106.5682>
- N. M. Kuznetsov, D. Y. Stolyarova, S. I. Belousov, et al., *Express Polym. Lett.* **12**, 958 (2018).  
<https://doi.org/10.3144/expresspolymlett.2018.82>
- N. M. Kuznetsov, S. I. Belousov, R. A. Kamyshinsky, et al., *Carbon* **174**, 138 (2021).  
<https://doi.org/10.1016/j.carbon.2020.12.014>
- O. Quadrant and J. Stejskal, *J. Ind. Eng. Chem.* **12**, 352 (2006).  
<http://www.scopus.com/inward/record.url?eid=2-s2.0-33744812017&partnerID=40&md5=589a9e57c32a404d5744fdbf2a2d0ccb>
- K. Choi, C. Y. Gao, J. D. Nam, and H. J. Choi, *Materials* **10**, 1060 (2017).  
<https://doi.org/10.3390/ma10091060>
- R. J. Moon, A. Martini, J. Nairn, et al., *Chem. Soc. Rev.* **40**, 3941 (2011).  
<https://doi.org/10.1039/c0cs00108b>
- M. Barikani, E. Oliaei, H. Seddiqi, and H. Honarkar, *Iran. Polym. J. (Engl. Ed.)* **23**, 307 (2014).  
<https://doi.org/10.1007/s13726-014-0225-z>
- O. I. Bogdanova and S. N. Chvalun, *Polymer Sci., Ser. A* **58**, 629 (2016).  
<https://doi.org/10.1134/S0965545X16050047>
- Y. G. Ko, S. S. Shin, U. S. Choi, et al., *ACS Appl. Mater. Interfaces* **3**, 1289 (2011).  
<https://doi.org/10.1021/am200091r>
- N. M. Kuznetsov, Y. D. Zagoskin, A. Y. Vdovichenko, et al., *Carbohydr. Polym.* **256**, 117530 (2021).  
<https://doi.org/10.1016/j.carbpol.2020.117530>
- N. M. Kuznetsov, Y. D. Zagoskin, A. V. Bakirov, et al., *ACS Sustain. Chem. Eng.* **9**, 3802 (2021).  
<https://doi.org/10.1021/acssuschemeng.0c08793>
- T. Blythe and D. Bloor, *Electrical Properties of Polymers* (Cambridge Univ. Press, Cambridge, 2005).
- T. E. Grigoriev, Y. D. Zagoskin, S. I. Belousov, et al., *Bionanosci.* **7**, 492 (2017).  
<https://doi.org/10.1007/s12668-017-0411-5>
- A. V. Vasilyev, T. B. Bukharova, V. S. Kuznetsova, et al., *Inorg. Mater. Appl. Res.* **10**, 1093 (2019).  
<https://doi.org/10.1134/S2075113319050332>
- R. J. Harris, in *Electron Microscopy Methods and Protocols*, Ed. by M. A. N. Hajibagheri (Humana Press, New York, 1999), p. 13.  
<https://doi.org/10.1385/1-59259-201-5:13>
- L. C. Davis, *J. Appl. Phys.* **72**, 1334 (1992).  
<https://doi.org/10.1063/1.351743>
- L. C. Davis, *J. Appl. Phys.* **81**, 1985 (1997).  
<https://doi.org/10.1063/1.364231>
- A. Y. Vdovichenko, N. M. Kuznetsov, V. G. Shevchenko, et al., *Diamond Relat. Mater.* **107**, 107903 (2020).  
<https://doi.org/10.1016/j.diamond.2020.107903>
- K. Y. Shin, S. Lee, S. Hong, and J. Jang, *ACS Appl. Mater. Interfaces* **6**, 5531 (2014).  
<https://doi.org/10.1021/am405930k>

Translated by M. Batrukova